Heliyon 9 (2023) e22522

Contents lists available at ScienceDirect

Heliyon

journal homepage: www.cell.com/heliyon

Modeling ultrasound modulation of neural function in a single cell

Heba M. Badawe, Rima H. El Hassan, Massoud L. Khraiche *

Neural Engineering and Nanobiosensors Group, Biomedical Engineering Program, Maroun Semaan Faculty of Engineering and Architecture, American University of Beirut, Beirut, Lebanon

ARTICLE INFO

Keywords:
Ultrasound
LIFUS
Neuromodulation
HH neuron
Firing rate
Latency
Action potential amplitude

ABSTRACT

Background: Low intensity ultrasound stimulation has been shown to non-invasively modulate neural function in the central nervous system (CNS) and peripheral nervous system (PNS) with high precision. Ultrasound sonication is capable of either excitation or inhibition, depending on the ultrasound parameters used. On the other hand, the mode of interaction of ultrasonic waves with the neural tissue for effective neuromodulation remains ambiguous.

New method: Here within we propose a numerical model that incorporates the mechanical effects of ultrasound stimulation on the Hodgkin-Huxley (HH) neuron by incorporating the relation between increased external pressure and the membrane induced tension, with a stress on the flexoelectric effect on the neural membrane. The external pressure causes an increase in the total tension of the membrane thus affecting the probability of the ion channels being open after the conformational changes that those channels undergo.

Results: The interplay between varying the acoustic intensities and frequencies depicts different action potential suppression rates, whereby a combination of low intensity and low frequency ultrasound sonication proved to be the most effective in modulating neural function.

***Comparison with Existing Methods*:** Our method solely depends on the HH model of a single neuron and the linear flexoelectric effect of the dielectric neural membrane, when under an ultrasound-induced mechanical strain, while varying the ion-channels conductances based on different sonication frequencies and intensities. We study the effect of ultrasound parameters on the firing rate, latency, and action potential amplitude of a HH neuron for a better understanding of the neuromodulation modality of ultrasound stimulation (in the continuous and pulsed modes).

Conclusions: This simulation work confirms the published experimental data that low intensity and low frequency ultrasound sonication has a higher success rate of modulating neural firing.

1. Introduction

Ultrasound neuromodulation is a promising therapeutic tool to non-invasively stimulate deep brain regions. With a high spatial and temporal resolution, ultrasonic neurostimulation can target the CNS [1,2], and PNS [3–5] to induce neural attenuations. Ultrasound waves interact with the tissues resulting in either excitation or inhibition of the neural function. Principally, ultrasound waves are mechanical vibrations with frequencies above the human hearing range (20 Hz–20 kHz). These acoustic waves of pressure propagate through compressible media by inducing media particle vibrations and pressure variations. Such waves can be reflected, refracted, diffracted, and scattered depending on the properties of the propagating medium [6]. The frequency of ultrasound waves is specified

* Corresponding author.
E-mail address: mkhraiche@aub.edu.lb (M.L. Khraiche).

https://doi.org/10.1016/j.heliyon.2023.e22522
Received 20 June 2022; Received in revised form 10 October 2023; Accepted 14 November 2023
Available online 21 November 2023

by the carrier frequency of the ultrasound transducer used to deliver those waves. Frequency determines wave absorption by the target tissue and the focal area range [7]. The intensity of ultrasound waves specifies the power of the sound wave and is measured by the average power per cross-sectional area. For a sinusoidal acoustic wave, the average intensity is proportional to the square of the applied pressure with $I = p^2(t)/2\rho c$, where p (t) is the pressure input, ρ is the density of the propagation medium, and c is the speed of sound in that medium [7–9,8].

Ultrasound sonication has many biophysical effects on tissues of interest and thus can induce various outcomes. Low intensity, low frequency ultrasound has shown promising results for the reversible modulation of deep brain regions and enhancement of neuronal activity [10]. Low intensity focused ultrasound (LIFUS) can alter brain activity when targeting cortical and subcortical regions in mammals [11]. Add to that, focused ultrasound stimulation can depolarize neurons in invertebrate animals like the medicinal leech [12]. Back in 2008, Tyler et al. proved the capability of LIFUS on exciting the central neurons of *ex vivo* mice brains [13]. The neurons showed an elevated synaptic transmission leading to a heightened inward flux of the positive sodium and calcium ions which generated a train of action potentials. Following this, many studies investigated the efficacy of different ultrasound parameters on neuromodulation [13–16]. Some emphasized the suppression activity of ultrasound, whereby LIFUS suppressed visually evoked potentials in rats after light stimulation [17], as well as inhibited seizures in epileptic monkeys with the use of 800 kHz ultrasound waves for a sonication time of 15 min [18]. On the other hand, pulsed ultrasound of 800 kHz frequency was shown to excite auditory cortical neurons using *c*-Fos staining [19]. Recently, Yoo et al. used 300 kHz continuous ultrasound waves to excite cortical neurons of rats in culture while measuring the increase of calcium accumulation inside the cells [20]. The impact of ultrasound, being excitation or suppression, might be a result of the sonication duration and the overall ultrasound parameters used. With short duty cycles and longer sonication durations, ultrasound waves delivered to the M1 cortical region in humans suppressed activity after excitation using transcranial magnetic stimulation (TMS) [21]. That specific combination of ultrasound parameters mostly yielded neural inhibition in mammals [16,17,21–23,]. Using the *Aplysia californica* model, Jordan et al. [24] succeeded in using different sonication frequencies to stimulate an isolated *Aplysia* abdominal ganglion and obtained comparable results with applied electrical stimulation. While typical low intensity ultrasound parameters failed to induce compound action potentials in unmyelinated crab leg nerve bundles, Wright et al. reported successful ultrasound stimulation at high intensities through inertial cavitation activity [25].

Ultrasound waves can be delivered in a continuous or pulsed mode. Continuous ultrasound waves are generated with a constant amplitude due to the continuous electrical excitation of the ultrasound transducer with a constant amplitude sinusoidal wave. On the other hand, pulsed ultrasound waves are generated with varying amplitude due to the consistently spaced on-and-off electrical excitations of the transducer with electrical signals of limited lengths. Those waves are delivered with a constant duty cycle as repeated tone bursts [26] thus inducing several discrete mechanical events in tissues. Kim et al. studied the effect of varying the sonication parameters, mainly the duty cycle, on the excitation capabilities of ultrasound waves on the somatomotor area of the rat brain [27]. They showed that pulsed ultrasound waves caused less tissue heating and achieved better neural stimulation with lower acoustic intensities and power disposition. Yet, another study demonstrated that pulsed ultrasound waves are as effective as continuous ultrasound waves with a slight preference for using continuous waves at high intensities for an enhanced neural excitation response [14]. Interestingly however, the same study showed that duty cycles beyond 60 % significantly increased the success rate of pulsed ultrasound sonication.

The mechanism of action by which ultrasound interacts with a neural tissue is still a topic of debate, mainly due to the plethora of physical effects of ultrasound on the cellular and subcellular components of biological tissues [28]. Thermodynamical and mechanical stimulation induced by ultrasound waves creates biophysical forces that affect neuronal signaling [28–30,29]. Ultrasonic negative pressure during the rarefaction phase of an acoustic wave propagation might cause bubble formation and cavitation [31], along with some large-scale axonal deformations accompanied with some thermal transformations [31–33]. Note that Menz et al. [34] reported ultrasound-induced acoustic radiation forces which transferred their momentum onto the neural membrane, causing mechanical displacement of the membrane of retinal slices *in vivo*. Nonetheless, the more robust the force applied, the higher the exerted pressure on the neural membrane. This pressure stimulus activates the mechano-sensitive ion channels, hence increasing the accumulation of positive ions, especially Ca^{2+}, in the intracellular medium [[20]. Consequently, a burst of action potential firing is generated. The mechanical strain applied to the neural membrane might change the natural distribution of its dipole moments, leading to surface polarization known as direct flexoelectricity of the biological tissue [34–37]. The flexoelectric effect can modulate the stress-sensitive channels promoting membrane depolarization [38]. Changing ultrasound sonication parameters can in turn change the mode of action of ultrasound [39]. Delivering focused ultrasound waves to freely moving *C. elegans nematodes* emphasized the importance of mechanosensitive ion channels to elicit a neural response manifested with increased avoidance while knocking down the thermosensitive ion channels rendered the neural response unaffected [40]. Previously, Wells [41] showed that ultrasound waves, when absorbed, transform into heat through friction. He argued that the higher the frequency, the better the absorption. However, King et al. proved the opposite [14]; whereby increasing ultrasound frequency caused a drop in the success rate when examining the mouse somatomotor response.

The mechano-electrical coupling of ultrasound with the neural membrane gave rise to multiple theoretical models that attempt to explain ultrasound neuromodulation. Following on the cavitation/sonoporation phenomenon, Krasovitski et al. introduced the bilayer sonophore model (BLS) which stresses the fact that the lipid bilayer neural membrane absorbs the acoustic pressure of ultrasound waves inducing extension and reduction of the intracellular space, thus causing membrane motion and action potential generation [31]. Plaksin et al. [41–43] developed the neuronal intramembrane cavitation excitation model (NICE) using the BLS model as its mechanical component and the Hodgkin-Huxley modified differential equations for the electrical component. Though computationally exhaustive, the interplay between these two parts allows the prediction of the neural response to ultrasound sonication. The SONIC model (multiscale optimized neuronal intramembrane cavitation model), developed by Lemaire et al. [43–45,44], overcomes the

computational difficulties and rigidity of the NICE model, allowing for enhanced exploration of the influence of multiple LIFUS parameters on the neural response. These models focus on the cavitation mode of action of ultrasound-tissue interaction and ignore other mechanisms by which ultrasonic waves might induce a neural response, including ion channel mechano-sensitivity [45–47] and direct and reverse flexoelectricity [48].

In this study, we design a numerical model that couples the mechanical effects of ultrasound to the Hodgkin-Huxley (HH) electrical model of a neuron. In particular, the flexoelectric effect of the dielectric neural membrane, following the ultrasound-induced mechanical strain, shapes the core of our modeling regime. Whereby flexoelectricity is the main contributor to the linear coupling between the membrane polarization and ultrasound-induced strain for neuromodulation. We investigate the impact of low ultrasound frequencies and intensities (in the continuous and pulsed modes) on multiple aspects of neuronal activity, including the firing rate, latency, and action potential amplitude of a HH neuron. We also report the potential optimal ultrasound parameters needed for efficient modulation of the neuronal response. By considering the amplitude suppression rate which calculates the percentage difference in action potential amplitude with no ultrasound sonication versus with ultrasound sonication, we study the effect of increasing ultrasound frequency and acoustic intensity on neural firing.

2. Materials and methods

2.1. Modeling the ultrasound transducer

The ultrasound transducer was modeled using the k-Wave open-source MATLAB toolbox. The toolbox is used for time-domain simulations of acoustic waves propagating in a 2 or 3-dimensional medium [49]. The model is based on the solution of first-order differential equations using a k-space pseudo-spectral method. Those equations govern the propagation of acoustic waves, through a compressible medium, under various conditions which cause dynamic fluctuations in the pressure and density of the medium, along with the acoustic particle velocity. Computations were carried out on a 64 by 64 2-D grid with a time step of 0.2 μs. The transducer was modeled as a straight line across the top of the grid, with a sensor mask covering the entire computational domain. The transducer received an input sinusoidal signal in the form of acoustic pressure ($p = P_m \sin(2\pi ft)$), where P_m represents the pressure amplitude and f the carrier frequency. The input acoustic pressure was converted to particle velocity, assigned in the x-direction, and propagating in the ultrasound gel medium of 987 kg/ m^3 density and at a speed of 1500 m/s. The output acoustic intensity was then calculated as a function of particle velocity and input acoustic pressure. The maximum intensity pixel was identified in the grid (at a distance of 12 mm from the face of the transducer) and pressure amplitude was computed at that focal point. Note that a perfectly matching layer was designed to prevent the waves hitting the edges of the domain from wrapping around and causing any reflection and noise. Using the maximum pressure and intensity obtained in the XY-plane, the beam pattern surrounding the focal point of the transducer is shown in Fig. 1.

2.2. Modeling the HH neuron

The neural membrane is a dielectric lipid bilayer that acts as a capacitor with variable resistance. The neural membrane contains multiple ion channels characterized with resistances specific to each type of ion crossing the membrane. Alan Hodgkin and Andrew Huxley's neuron model is a basic electrical circuit where the voltage-gated ion channels, mainly the sodium and potassium ion

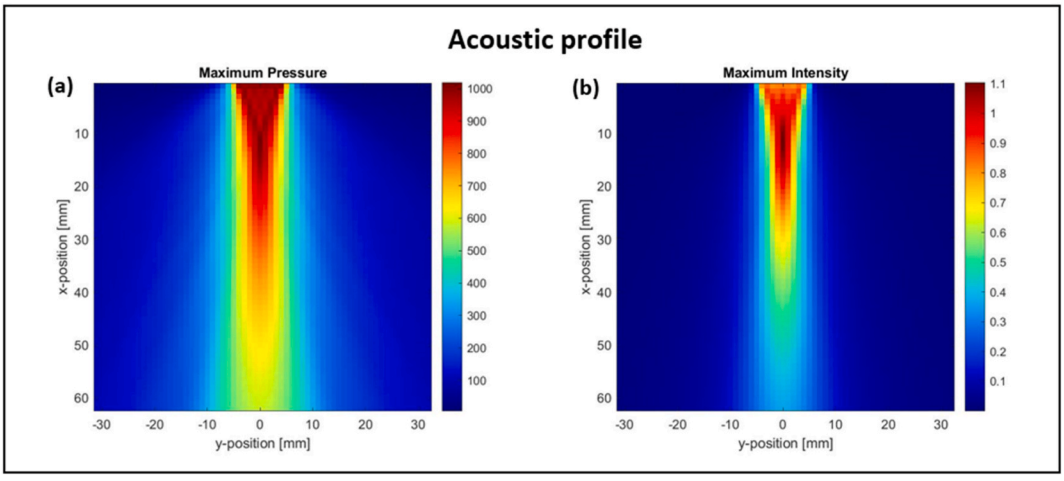

Fig. 1. Simulation of the acoustic profile of an ultrasound transducer of 350 kHz frequency and 1 MPa input acoustic pressure. The ultrasound transducer is modeled as a straight line across the top of the computational grid with its focal point being at a distance of 12 mm from the face of the transducer. (a) Simulated ultrasound pressure amplitude (in kPa) around the focal point in the XY plane. (b) Simulated maximum output acoustic intensity (in W/ cm^2) in the XY-plane.

channels, were represented by their electrical conductance g_{Na} and g_k respectively, along with some leak channels with linear conductance g_l [50]. The total current passing through the membrane is a summation of the capacitive current and the current traversing each ion channel:

$$I = C_m\left(\frac{dV_m}{dt}\right) + g_{Na}(V_m - V_{Na}) + g_k(V_m - V_k) + g_l(V_m - V_l)$$

where C_m is the membrane capacitance, V_m is the membrane potential and V_i is the i-th ion channel Nernst potential.

We modeled a firing neuron by introducing a minimal current of 6.3 mA, enough to depolarize the membrane potential above the threshold. As the action potential propagates along the neural membrane, a transient phase change of charges occurs [51]. This creates a strain gradient that affects the thickness of the membrane thus altering the conductance of the ion channels. Those events enhance the flexoelectricity of the neural membrane giving rise to a flexoelectric current via curvature-dependent polarization of the membrane (Fig. 2). This flexoelectric current depends on the flexoelectric voltage induced and capacitance of the neural membrane. As a consequence, a further change in the membrane potential ΔV_m is achieved which creates additional tension in the membrane of the neuron.

2.3. Coupling the ultrasound mechanical effects to the HH model

Ultrasound mechanical waves propagate through the neural membrane exerting pressure on a small segment of the membrane, thus inducing lateral tension [52]. Add to that, the flexoelectric current and the injected current give rise to a membrane-voltage induced tension. Adding this to the lateral tension yields a total membrane tension γ which proportionally changes the intrinsic internal energy difference ΔG as the ligand and voltage-gated ion channels go from the closed state to the open state [53]. This is due to the capacitive aspect of the lipid bilayer membrane, whereby the charges' mobility and redistribution impact γ [54]. The internal energy difference can be expressed as:

$$\Delta G = -\gamma \Delta a + \Delta u$$

where Δa represents the change in the channel's area as it opens, while Δu represents the intrinsic difference in energy between states with no applied tension.

The probability of the channels being open due to the total membrane tension γ can be expressed as:

$$P_0 = \frac{1}{1 + e^{\left(\frac{\Delta G}{\kappa_b T}\right)}}$$

where κ_b is the Boltzmann constant and T is the absolute temperature in Kelvin.

Notice that as ΔG decreases algebraically, P_0 increases. When channels open, they undergo conformational changes which increase

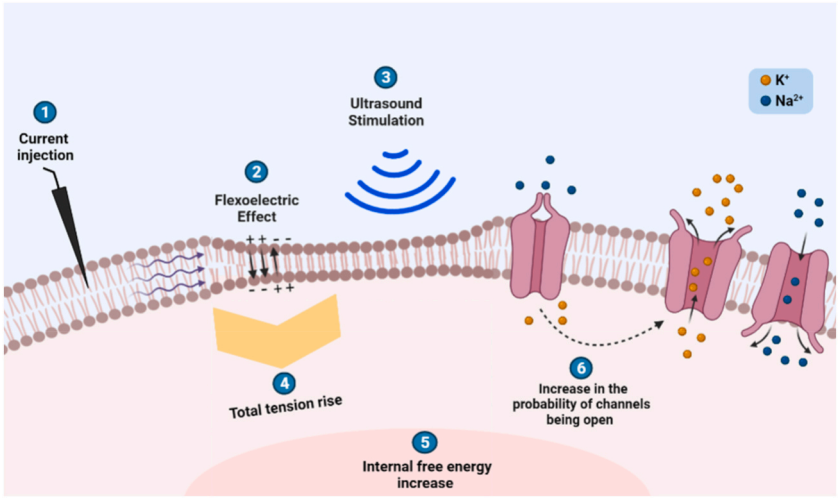

Fig. 2. Effect of ultrasound waves on a HH neuron. (1) Current is injected to mimic the natural firing of a HH neuron. The variation propagates throughout the neural membrane. Due to the membrane's dielectric nature, a transient phase change of charges creates a strain gradient which couples with a spontaneous electrical polarization and generates a flexoelectric current (2). This gives rise to a membrane-voltage induced tension. As ultrasound stimulation is applied (3), the pressure creates a lateral tension. (4) The total tension rise induces a change in the internal free energy ΔG which in turn increases the probability of the ion channels being open due to a change in their conductance (6). A noticeable increase in the outward potassium current supports the suppressive nature of ultrasound stimulation to a HH neuron.

their area Δa. This causes a decrease in ΔG, hence an increase in P_0. This alters the conductance of each ion channel accordingly. Note that the total tension γ, the membrane potential difference ΔV_m, and the change in ion channel conductance are all in a continuous feedback loop affecting the neural action potential firing (Fig. 3).

Our biomechanical model couples the mechanical effects of ultrasound represented by the flexoelectric current, and the consequent rise in the total membrane tension γ to the HH electrical model through changes in the conductance of ion channels. Upon ultrasound stimulation, the ion channels open in response to the corresponding gating variables in addition to the total induced tension. Whereby:

$$g_{Na} = \overline{G_{Na}} \times m^3 h \times P_0$$

$$g_K = \overline{G_K} \times n^4 \times P_0$$

$$g_l = \overline{G_l} \times P_0$$

where $\overline{G_{Na}}$, $\overline{G_K}$, and $\overline{G_l}$ are the maximal conductance of the sodium, potassium, and leak channels respectively, and n, m, and h

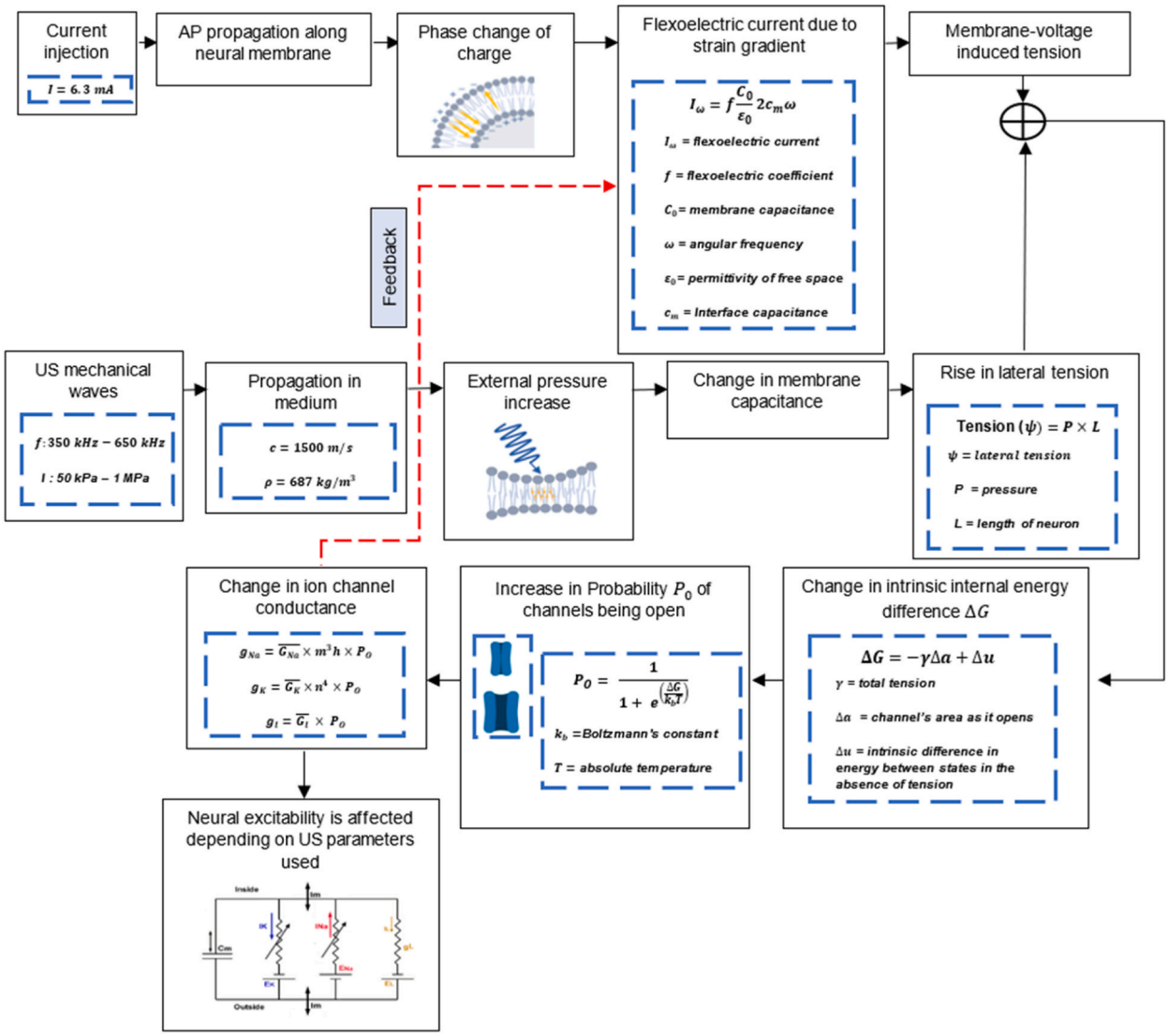

Fig. 3. Flow chart illustrating the model components. The injected current and the flexoelectric current generated from the viscoelastic nature of the lipid bilayer create a membrane-voltage induced tension. Adding the latter to the lateral tension induced by the external pressure generated from the ultrasound mechanical waves causes a change in the intrinsic energy difference. This increases the probability of ion channels being open thus changing their conductance. As a result, neural excitability is affected and manifested with different firing rates, latencies, and action potential amplitudes. Note that all the components are in a continuous feedback loop whereby a change in the conductance due to ultrasound waves affects the membrane potential which in turn produces a flexoelectric current.

represent the probability of potassium channel activation, sodium channel activation, and sodium channel inactivation respectively.

This way the probability of the ion channel being open depends on two aspects: the gating variables of the ion channels as normally presented in the HH equations of conductance, followed by the addition of the total tension rise in the neural membrane, presented by P_0, after ultrasound stimulation.

3. Results

3.1. Ultrasound stimulation of a single firing HH neuron

Ultrasound stimulation induces neural excitability. Varying the frequency and intensity of ultrasound vibrations affects the firing rate, latency, and peak-to-peak voltage (Vpp) of the neural action potential. We run simulations that increase the ultrasound frequency from 350 kHz to 650 kHz with a 100 kHz increment and increase the input acoustic pressure from 50 kPa to 1 MPa with a 50 kPa increment. Those simulations were run in two sets; Set 1 corresponds to the delivery of continuous ultrasound waves to a HH neuron while set 2 corresponds to the delivery of pulsed ultrasound waves (duty cycle of 50 % and tone burst duration of 2 m s). A HH neuron simulated with no alterations recorded a peak-to-peak voltage of 105 mV, a firing rate of 53.5 Hz, and a latency of 21 m s when injected with a 6.3 mA current to mimic natural firing. The effect of ultrasound stimulations (continuous and pulsed) on neural excitability was compared to the variations in the HH neuron when no ultrasound stimulations were applied.

3.2. Firing rate

Ultrasound stimulations induced an increase in the firing rate from 53.5 Hz to a range between 68.5 Hz and 75 Hz with continuous

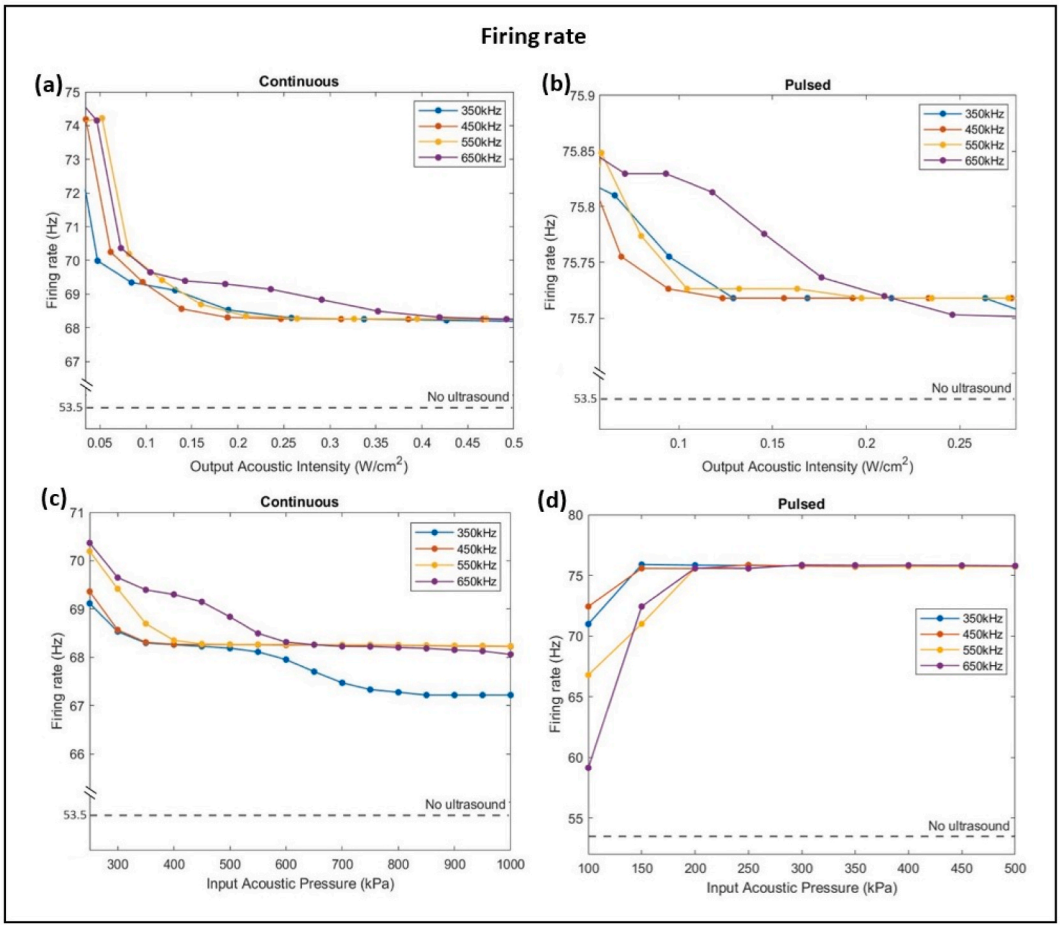

Fig. 4. Variation of firing rate with respect to frequency, acoustic intensity (a & b), and acoustic pressure (c & d) of ultrasound stimulation in both continuous and pulsed modes. Increasing the acoustic intensity causes a decrease in firing rate to lower values of 67 Hz with continuous ultrasound waves (a) than with pulsed waves of 75.7 Hz (b). However, as the input pressure increases, the firing rate decreases to a minimum of about 67 Hz with continuous ultrasound waves (c), yet it increases to a maximum of 76 Hz with pulsed ultrasound waves (d). The dashed line represents the reference firing rate of a firing neuron when no ultrasound sonication was applied.

ultrasound stimulations (Fig. 4-a), while pulsed ultrasound stimulations showed an increase in firing rate values ranging between 75.7 Hz and 75.85 Hz (Fig. 4-b). As the output acoustic intensity increased, continuous and pulsed ultrasound neurostimulations caused a decrease in the firing rate to values still more than reference 53.5 Hz. Major attenuations in the firing rate occurred at low acoustic intensities (less than 0.1 W/ cm^2) where higher frequencies resulted in higher firing rates. For set 1, increasing the intensity past 0.45 W/ cm^2 had no further effect on the firing rate. It was noticeable that increasing the input acoustic pressure caused a decrease in the firing rate in set 1 (Fig. 4-c) while it caused an increase in set 2 (Fig. 4-d), with more attenuation seen at lower acoustic pressures. Pulsed ultrasonic stimulations had no further effect on the firing rate beyond 300 kPa. Moreover, a low input acoustic pressure of 200 kPa resulted in the highest firing rates for both sets.

3.3. Latency

The frequency and intensity of ultrasonic stimulations affect the time between stimulation and response of the neuron. Ultrasound stimulations caused a decrease in the latency in both sets, whereby continuous ultrasound waves decreased the latency from reference 21 m s to a range between 17.9 m s and 18.35 m s (Fig. 5-a), while pulsed ultrasound waves decreased the latency to approximately 18.43 m s (Fig. 5-b). As the output acoustic intensity increased, ultrasound stimulations increased the latency from 17.9 m s to 18.35 m s in set 1, while in set 2 they decreased the latency from 18.55 m s to 18.43 m s. Add to that, attenuations majorly occurred at lower acoustic intensities, whereby continuous ultrasonic stimulations caused no further increase in latency beyond 0.45 W/ cm^2. Ultimately, in both sets, ultrasound stimulations had little effect on the latency.

3.4. Action potential amplitude

In a HH neuron, the action potential amplitude, measured from the minimal peak at hyperpolarization to the maximal peak at depolarization, was 105 mV. Upon ultrasound stimulation, the action potential amplitude dropped to a range between 84 mV and 98 mV with continuous ultrasound (Fig. 6-a) and a lower range between 66 mV and 74 mV with pulsed ultrasound stimulations (Fig. 6-b). Increasing the acoustic intensity caused an increase in the peak-to-peak voltage for both sets to values still less than the reference Vpp with no ultrasound sonication. The smaller the acoustic intensities applied, the more attenuation in Vpp was noticed; Whereby continuous ultrasound stimulations caused no noticeable Vpp increase past 0.5 W/ cm^2. Moreover, lower frequencies implemented a higher drop in the peak-to-peak voltage. A similar pattern was recorded as the input acoustic pressure increased (Fig. 6 c & d). Both sets of simulations showed no further change in Vpp as the input pressure increased beyond 600 kPa. The results demonstrated that pulsed ultrasound stimulations were more successful in suppressing the action potential amplitude causing more modulation of a single neuron firing especially at lower acoustic intensities. The drop in action potential amplitude after sonication was emphasized by the amplitude suppression rate which was the highest of 16.3 % at 350 kHz frequency and 0.04 W/ cm^2 intensity, and lowest of 6.7 % at 650 kHz frequency and 0.6 W/ cm^2 intensity (Fig. 7).

3.5. Output acoustic intensity

Ultrasound frequency and the output acoustic intensity are inversely proportional (Fig. 8-a). With more pressure being applied to the single HH neuron, lower frequencies showed higher values of output acoustic intensities. As the frequency varied from 350 kHz to

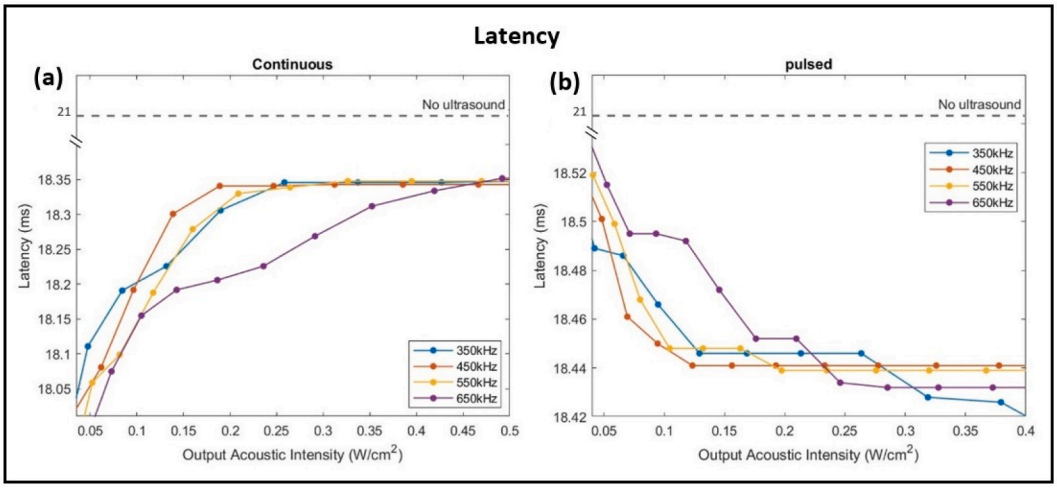

Fig. 5. Effect of acoustic intensity and frequency on the latency of the neural response. Increasing the intensity caused an increase in latency to a maximum of 18.35 m s with continuous ultrasound waves yet it caused a decrease in latency to a minimum of 18.43 m s with pulsed ultrasound waves. The dashed line represents the reference latency of a firing neuron when no ultrasound sonication was applied.

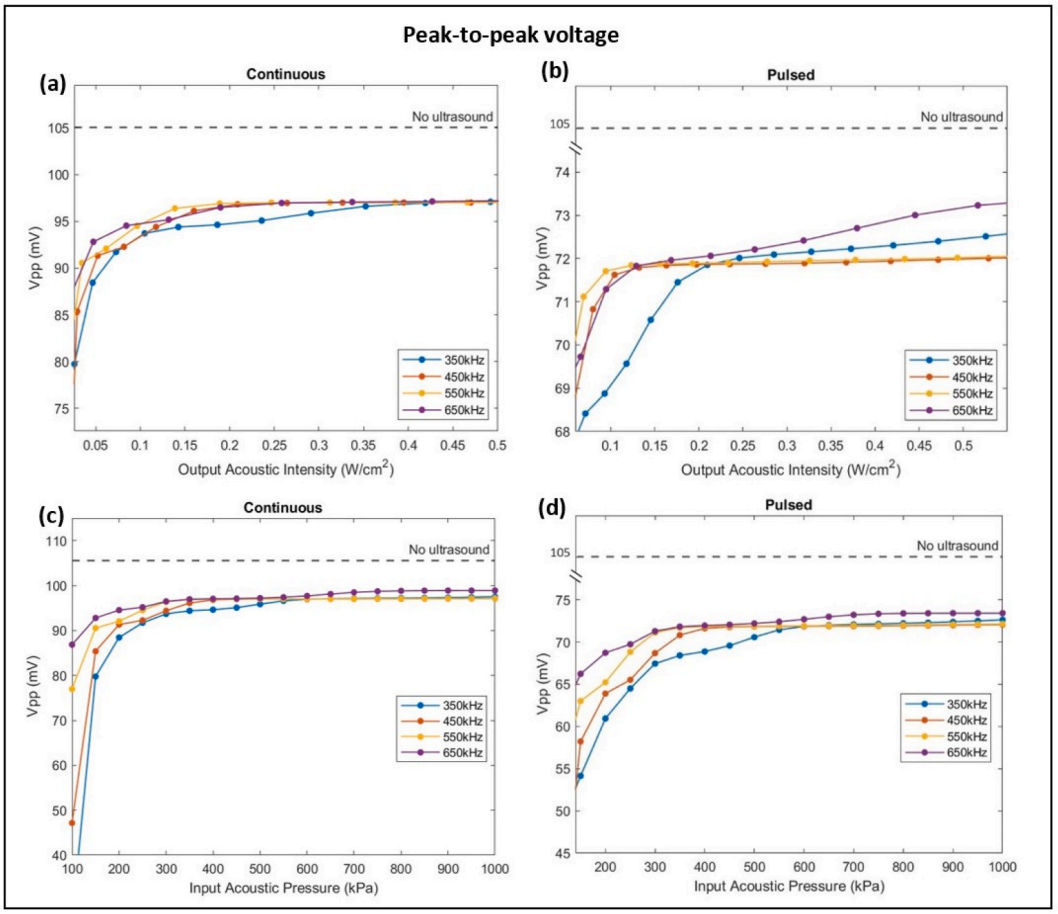

Fig. 6. Variation of peak-to-peak voltage as a function of frequency, acoustic intensity (a & b), and input acoustic pressure (c & d) of ultrasound stimulation in both continuous and pulsed modes. Pulsed ultrasound waves suppress the action potential amplitude to a lower range of 66 mV–74 mV while continuous ultrasound waves decrease the amplitude to a range of 84 mV–98 mV. Increasing the input acoustic pressure beyond 600 kPa has no further effect on Vpp. The dashed line represents the reference Vpp of a firing neuron when no ultrasound sonication was applied.

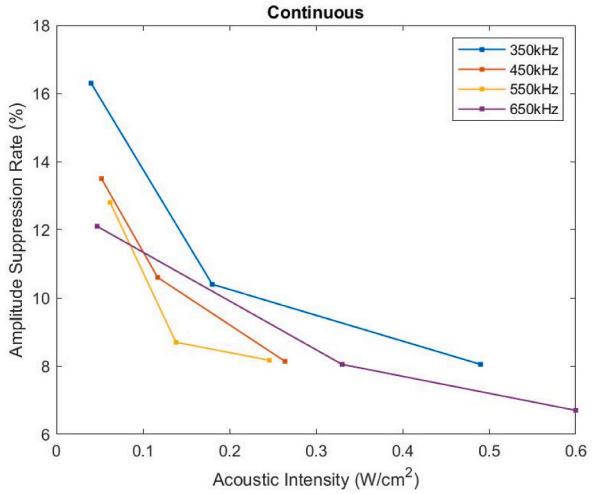

Fig. 7. Continuous ultrasound sonication suppresses the action potential firing leading to a drop in the action potential amplitude as a function of frequency and acoustic intensity. At lower frequencies and lower acoustic intensities, the amplitude suppression rate reaches its maximum.

650 kHz, more input acoustic pressure was required to induce neural excitability. Higher output acoustic intensities were reached with set 1 simulation in comparison with set 2 simulations. The results showed that at lower frequencies, continuous ultrasound stimulations can produce higher output acoustic intensities with lower input acoustic pressure than pulsed ultrasound stimulations. Moreover, the threshold acoustic intensity required to induce changes in neural excitability decreased as the frequency increased (Fig. 8-b).

4. Discussion

Ultrasound has emerged as a promising neuromodulation modality that can, noninvasively, excite or inhibit neural pathways depending on the parameters used. The mechanism by which ultrasound can interact with the neural membrane to generate or suppress an action potential is still not well understood. Acoustic perturbations can cause conformational changes in the neural membrane, thus altering the membrane capacitance, opening of ion channels, flexoelectricity, and thermal state of the membrane which can all contribute to neurostimulation [55]. Thermal energy generation or bubble formation and cavitation are not primary causes for action potential modulation when using LIFUS in the parameter ranges we opted for [20]. Yet, mechanical ultrasound waves exert pressure on the membrane of the single neuron causing mechanical deformations to the actin cytoskeletons [56]. This increases the lateral tension proportionally to the increase in the input pressure. Mechanical stress modulates the behavior of the mechanosensitive transmembrane proteins and ion channels embedded throughout the neural membrane, thus altering the ion distribution across the membrane. Therefore, we developed a model that simulates the effects of ultrasound stimulations, in the continuous and pulsed modes, on the neural membrane potential and subsequent neural excitability.

The model incorporated mechanical components into the typical electrical HH model of a neuron. Those mechanical components consisted of the membrane tension and the linear flexoelectric effect of the viscoelastic lipid bilayer membrane that induced a change in the probability of the ion channels being open due to ultrasound stimulations (Fig. 2). The model displayed the neuromodulatory action of ultrasound stimulations, continuous and pulsed, on the suppression of the action potential amplitude and modulation of the firing rate and latency. Add to that, the model investigated the effect of increasing the frequency and input acoustic pressure on neural excitability. We studied the optimal parameters needed for the highest modulation of the activity of a firing HH neuron.

4.1. *Ultrasound sonication increases the firing rate*

Low intensity focused ultrasound stimulations on primary hippocampal neurons induced a major increase in firing and bursting rates when compared to the neuron's natural spontaneous activity [57]. Our model showed an increase in the firing rate with all ultrasound frequencies applied. Yet, at lower acoustic intensities, the highest firing rates were achieved, given that the latency and inter-stimulus-interval (ISI) recorded their lowest values, in contrast with higher acoustic intensities which caused a drop in the firing rate as the latency gradually increased. Lin et al. demonstrated that ultrasound mechanical waves applied to hippocampal pyramidal neurons *in-vitro* affected the opening of potassium channels [58]. This caused an increase in the diffusion of potassium ions outside the cell. Such maintained potassium conductance at higher input currents altered the shape of the action potential and depicted a faster repolarization stage. This limited any further hyperpolarization due to a smaller refractory period and a faster activation of the voltage-gated sodium channels. Prieto et al. showed that at lower acoustic intensities and higher frequencies, ultrasound potentiated

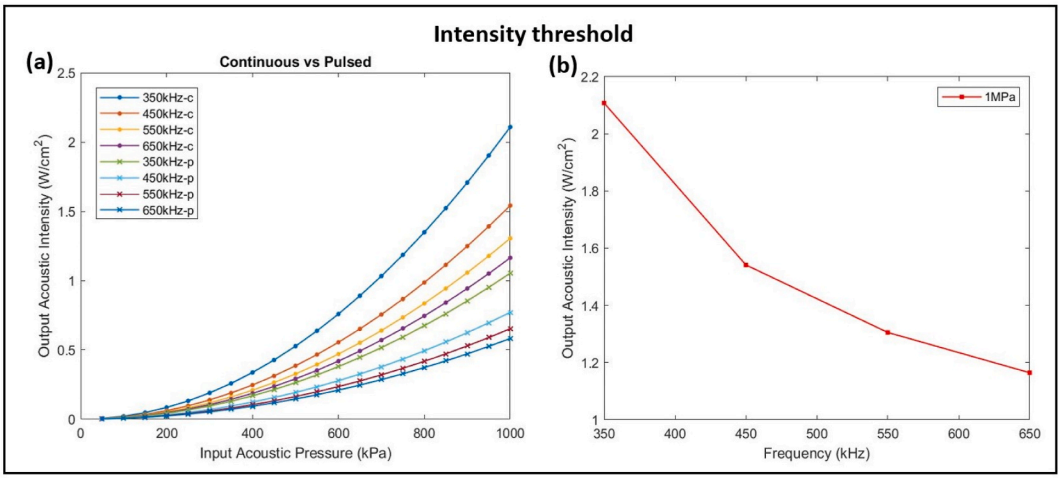

Fig. 8. Threshold acoustic intensity required to induce changes in neural excitability for low frequency US stimulation. (a) Variation of output acoustic intensity as a function of input acoustic pressure for continuous ultrasound (-c) and pulsed ultrasound (-p) at different frequencies. Frequency and output acoustic intensity are inversely proportional whereby higher frequencies generate less output intensity, and continuous ultrasound stimulation produces higher intensities than pulsed stimulation. (b) Output acoustic intensity as a function of increasing frequency at 1 MPa of input acoustic pressure.

firing. Whereas at higher acoustic intensities and lower frequencies, the effects were reversed, whereby a deeper hyperpolarization and an increase in the refractory period were noticed, thus decreasing the firing rate [59]. Knowing that intensity is proportional to the pressure applied, at lower input pressure of around 200 kPa, ultrasound stimulations, in the continuous and pulsed modes, induced the highest firing rates.

4.2. Ultrasound sonication decreases stimulation latency

The latency drop due to ultrasound stimulations was minute along with the (ISI). Overall, the mechanical waves caused a total decrease of 3 m s in the latency. Since ultrasound increased the firing rate of the HH neuron, the time between subsequent spikes decreased from 19 m s without ultrasound application to around 14 m s with ultrasound (Fig. 9). Cui et al. [60] recorded a significant decrease in the EMG response latency when the primary motor cortex of healthy mice was subjected to ultrasound acoustic pressures of 120 kPa and 250 kPa. Similarly, LIFUS targeted at the somatosensory cortex of mice recorded a decrease in the latency of sensory-evoked neural responses of 3 ± 0.7 m s [61]. Comparing the two sets of simulations, set 2 of our model showed a negligible decrease in latency with pulsed ultrasound stimulations (about 0.1 m s) as the acoustic intensity increased. Whereas set 1 showed a wider range of 0.45 m s difference as the acoustic intensity changed from 0.05 W/ cm^2 to 0.5 W/ cm^2.

4.3. Ultrasound sonication suppresses action potential amplitude

Ultrasound vibrations depolarized the resting membrane potential causing a shorter hyperpolarization and a smaller maximal membrane potential (Fig. 9). The peak-to-peak voltage dropped with both sets of experiments with an apparent higher suppression using pulsed sonication. The suppression of the action potential amplitude could be a consequence of the faster repolarization of the membrane potential. Colucci et al. [62] recorded a substantial reduction in action potential amplitude as the sciatic nerve of a bullfrog was subjected to a 661 kHz ultrasound sonication for 30 s. The results were in line with the outcomes of experiments performed by Juan et al. [63] where action potential inhibition was detected with the application of focused pulsed ultrasound to the vagus nerve of rats. Another simulation study investigated the effect of transcranial focused ultrasound (of 500 kHz frequency) on the electrical activity of several types of cortical neurons based on their bursting and spiking behavior [64]. Whereby the membrane potential of those neurons dropped significantly upon ultrasound simulation. Moreover, our model demonstrated an enhancement in the suppression effect of ultrasound as the acoustic intensity and sonication frequency were decreased (Fig. 7). This neuromodulation dependence on the combination of low sonication intensity and frequency was highlighted in the work of Guo et al. [65] while suppressing the peripheral sciatic nerve activity. Plaksin et al. [42] also predicted the same trend with their simulation neuronal bilayer sonophore model to obtain similar success rates as the experimental results in Ref. [14].

4.4. Ultrasound sonication alters the threshold of neural excitability

The neural membrane has components of resistance and capacitance that are highly affected when subjected to external pressure. The more pressure applied, the smaller the distance between the two plates of the capacitor (represented by the two lipid layers of the neural membrane) which causes an increase in the capacitance. Howell et al. showed a decrease in the membrane capacitance as a function of increasing the frequency of ultrasonic vibrations [66]. Thus, to compensate for the loss in capacitance with higher frequencies, more input acoustic pressure was needed to induce neural excitability and achieve higher output acoustic intensity (Fig. 8-a). Add to that, higher ultrasound acoustic frequencies tend to diffract more in tissues which reduces the penetration impact of ultrasound waves [67]. King et al. [14] performed transcranial ultrasound stimulations on mice to study their somatomotor response to variable sonication frequencies (from 250 kHz to 600 kHz). They reported that for higher frequencies, higher acoustic intensities were needed to achieve the same success rate as with a combination of low frequency, low intensity ultrasound sonication. For better action potential amplitude suppression, Fig. 8-b demonstrated that at lower frequencies, the threshold acoustic intensity required to induce neural excitability was the highest.

5. Conclusion

Our model coupled the mechanical effects of ultrasound stimulations to the electrical HH model of a single neuron. The conductance of each ion channel was the main component affected by the external pressure applied. The results emphasized the neuromodulation action of ultrasound waves on a HH neuron. The amplitude of action potential and the latency separating the time between stimulation and neural response decreased upon sonication while the firing rate increased. Moreover, continuous ultrasound waves achieved less latency values at low intensities, yet pulsed ultrasound waves recorded less peak-to-peak voltages and higher firing rates. The model emphasized that low acoustic intensities and low sonication frequencies were more efficient at modulating neural firing. However, in the study of Prieto et al. [59], they showed that not only did ultrasound waves decrease the height of action potentials, but also caused a shrinkage in their width. Yet, our model did not explicitly show that. To better study the effect of ultrasound waves on the modulation of neural firing, the temperature rise, the calcium current, and the potential changes in the speed of sound due to changes in density must be taken into consideration and further included in the model. Note that our model presented a framework to predict the effect of LIFUS on a firing HH neuron by mainly investigating the aspect of flexoelectricity of the neural membrane. Possible alternative mechanisms of ultrasound neuromodulation were not taken into consideration. Ultrasound stimulation can potentially replace the currently available invasive neuromodulation techniques, without requiring any implanted wired or

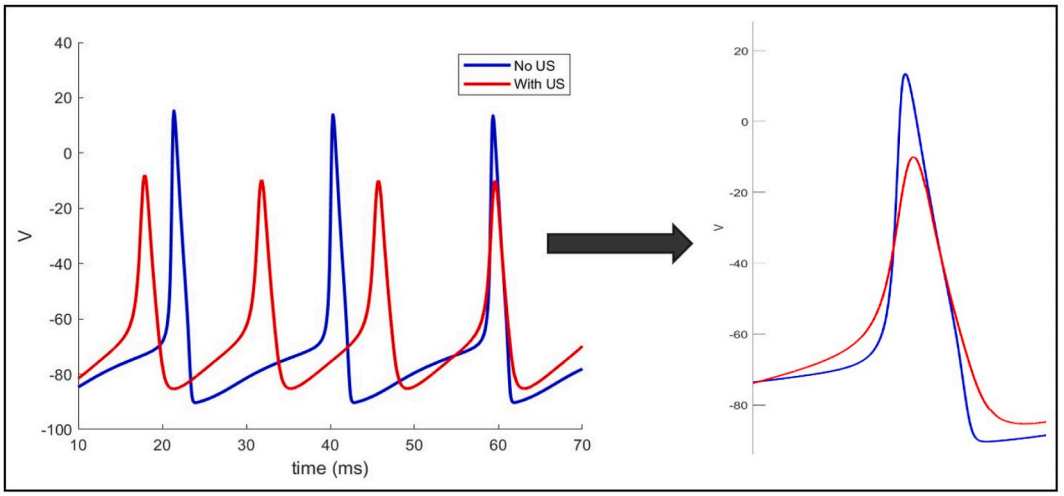

Fig. 9. Suppression of action potentials upon ultrasound stimulation. The blue trace represents the action potentials of a firing HH neuron with no ultrasound stimulation while the red trace corresponds to action potentials when ultrasound stimulation was applied. A firing HH neuron records higher amplitude, longer latency, and less firing rate than when subjected to ultrasound stimulation which induced a decrease in amplitude and latency and an increase in firing rate.

wireless components that bring several issues with safety and efficacy [67–69,68]. Hence, more simulation studies and modeling can help better understand the neural response as a function of varying ultrasound parameters for enhanced optimizations of neuromodulation.

CRediT authorship contribution statement

Heba M. Badawe: Data curation, Validation, Visualization, Writing – original draft, Writing – review & editing. **Rima H. El Hassan:** Formal analysis. **Massoud L. Khraiche:** Conceptualization, Formal analysis, Funding acquisition, Project administration, Supervision, Writing – original draft, Writing – review & editing.

Declaration of competing interest

The authors declare that they have no known competing financial interests or personal relationships that could have appeared to influence the work reported in this paper.

References

[1] K.-T. Chen, K.-C. Wei, H.-L. Liu, Theranostic strategy of focused ultrasound induced blood-brain barrier opening for CNS disease treatment, Front. Pharmacol. 10 (2019). Apr. 04, 2022. [Online]. Available: https://www.frontiersin.org/article/10.3389/fphar.2019.00086.
[2] M.L. Khraiche, N. Jackson, J. Muthuswamy, Early onset of electrical activity in developing neurons cultured on carbon nanotube immobilized microelectrodes, Conf. Proc. IEEE Eng. Med. Biol. Soc. 2009 (2009) 777–780, https://doi.org/10.1109/IEMBS.2009.5333590.
[3] R.H.E. Hassan, N.B. Lawand, E.D. Al-Chaer, M.L. Khraiche, Frequency dependent, reversible focused ultrasound suppression of evoked potentials in the reflex arc in an anesthetized animal, J. Peripher. Nerv. Syst. (Oct. 2022), https://doi.org/10.1111/JNS.12512.
[4] B. Feng, L. Chen, S.J. Ilham, A review on ultrasonic neuromodulation of the peripheral nervous system: enhanced or suppressed activities? Appl. Sci. Basel Switz. 9 (8) (Apr. 2019) 1637, https://doi.org/10.3390/app9081637.
[5] V. Cotero, et al., Peripheral focused ultrasound neuromodulation (pFUS), J. Neurosci. Methods 341 (Jul. 2020), 108721, https://doi.org/10.1016/j.jneumeth.2020.108721.
[6] D.P. Darrow, Focused ultrasound for neuromodulation, Neurotherapeutics 16 (1) (Jan. 2019) 88–99, https://doi.org/10.1007/s13311-018-00691-3.
[7] M. Heba, Badawe, Petra Raad, and Massoud L. Khraiche, "High Resolution Acoustic Mapping of Gelatin-Based Soft Tissue Phantoms," bioRxiv, Jan. 2023, https://doi.org/10.1101/2023.05.10.540075, 2023.05.10.540075.
[8] R.E. Hassan, T.E. Chemaly, M. Khraiche, Towards A biomechanical model for ultrasound effect on neural excitability, 2018 IEEE Int. Multidiscipl. Conf. Eng. Technol. IMCET 2018 (Jan. 2019), https://doi.org/10.1109/IMCET.2018.8603025.
[9] D.Q. Truong, C. Thomas, B.M. Hampstead, A. Datta, Comparison of transcranial focused ultrasound and transcranial pulse stimulation for neuromodulation: a computational study, Neuromodulation Technol. Neural Interf. (Feb. 2022), https://doi.org/10.1016/j.neurom.2021.12.012.
[10] H. Baek, K.J. Pahk, H. Kim, A review of low-intensity focused ultrasound for neuromodulation, Biomed. Eng. Lett. 7 (2) (May 2017) 135–142, https://doi.org/10.1007/s13534-016-0007-y.
[11] A. Fomenko, C. Neudorfer, R.F. Dallapiazza, S.K. Kalia, A.M. Lozano, Low-intensity ultrasound neuromodulation: an overview of mechanisms and emerging human applications, Brain Stimul. 11 (6) (Dec. 2018) 1209–1217, https://doi.org/10.1016/j.brs.2018.08.013.
[12] M.N. Collins, K.A. Mesce, Focused ultrasound neuromodulation and the confounds of intracellular electrophysiological investigation, eNeuro 7 (4) (Jul. 2020), https://doi.org/10.1523/ENEURO.0213-20.2020.
[13] W.J. Tyler, Y. Tufail, M. Finsterwald, M.L. Tauchmann, E.J. Olson, C. Majestic, Remote excitation of neuronal circuits using low-intensity, low-frequency ultrasound, PLoS One 3 (10) (Oct. 2008) e3511, https://doi.org/10.1371/journal.pone.0003511.

[14] R.L. King, J.R. Brown, W.T. Newsome, K.B. Pauly, Effective parameters for ultrasound-induced in vivo neurostimulation, Ultrasound Med. Biol. 39 (2) (Feb. 2013) 312–331, https://doi.org/10.1016/j.ultrasmedbio.2012.09.009.
[15] J. Blackmore, S. Shrivastava, J. Sallet, C.R. Butler, R.O. Cleveland, Ultrasound neuromodulation: a review of results, mechanisms and safety, Ultrasound Med. Biol. 45 (7) (Jul. 2019) 1509–1536, https://doi.org/10.1016/j.ultrasmedbio.2018.12.015.
[16] M.L. Khraiche, W.B. Phillips, N. Jackson, J. Muthuswamy, Sustained elevation of activity of developing neurons grown on polyimide microelectrode arrays (MEA) in response to ultrasound exposure, Microsyst. Technol. 23 (8) (Aug. 2017) 3671–3683, https://doi.org/10.1007/S00542-016-3150-6/FIGURES/10.
[17] H. Kim, M.Y. Park, S.D. Lee, W. Lee, A. Chiu, S.-S. Yoo, Suppression of EEG visual-evoked potentials in rats via neuromodulatory focused ultrasound, Neuroreport 26 (4) (Mar. 2015) 211–215, https://doi.org/10.1097/WNR.0000000000000330.
[18] J. Zou, et al., Ultrasound neuromodulation inhibits seizures in acute epileptic monkeys, iScience 23 (5) (May 2020), 101066, https://doi.org/10.1016/j.isci.2020.101066.
[19] X. Qi, et al., Low-intensity ultrasound causes direct excitation of auditory cortical neurons, Neural Plast. 2021 (Apr. 2021), e8855055, https://doi.org/10.1155/2021/8855055.
[20] S. Yoo, D.R. Mittelstein, R.C. Hurt, J. Lacroix, M.G. Shapiro, Focused ultrasound excites cortical neurons via mechanosensitive calcium accumulation and ion channel amplification, Nat. Commun. 13 (1) (Jan. 2022) 493, https://doi.org/10.1038/s41467-022-28040-1.
[21] A. Fomenko, et al., Systematic examination of low-intensity ultrasound parameters on human motor cortex excitability and behavior, Elife 9 (Nov. 2020), e54497, https://doi.org/10.7554/eLife.54497.
[22] S.-S. Yoo, et al., Focused ultrasound modulates region-specific brain activity, Neuroimage 56 (3) (Jun. 2011) 1267–1275, https://doi.org/10.1016/j.neuroimage.2011.02.058.
[23] W. Legon, et al., Transcranial focused ultrasound modulates the activity of primary somatosensory cortex in humans, Nat. Neurosci. 17 (2) (Feb. 2014), https://doi.org/10.1038/nn.3620. Art. no. 2.
[24] T. Jordan, J.M. Newcomb, M.B. Hoppa, G.P. Luke, Focused ultrasound stimulation of an ex-vivo Aplysia abdominal ganglion preparation, J. Neurosci. Methods 372 (Apr. 2022), 109536, https://doi.org/10.1016/j.jneumeth.2022.109536.
[25] C.J. Wright, S.R. Haqshenas, J. Rothwell, N. Saffari, Unmyelinated peripheral nerves can Be stimulated in vitro using pulsed ultrasound, Ultrasound Med. Biol. 43 (10) (Oct. 2017) 2269–2283, https://doi.org/10.1016/j.ultrasmedbio.2017.05.008.
[26] W.D. O'Brien, Ultrasound-biophysics mechanisms, Prog. Biophys. Mol. Biol. 93 (1–3) (Apr. 2007) 212–255, https://doi.org/10.1016/j.pbiomolbio.2006.07.010.
[27] H. Kim, A. Chiu, S.D. Lee, K. Fischer, S.-S. Yoo, Focused ultrasound-mediated non-invasive brain stimulation: examination of sonication parameters, Brain Stimul. 7 (5) (Oct. 2014) 748–756, https://doi.org/10.1016/j.brs.2014.06.011.
[28] J. Dell'Italia, J.L. Sanguinetti, M.M. Monti, A. Bystritsky, N. Reggente, Current state of potential mechanisms supporting low intensity focused ultrasound for neuromodulation, Front. Hum. Neurosci. 16 (2022), 872639, https://doi.org/10.3389/fnhum.2022.872639.
[29] G. ter Haar, Ultrasound bioeffects and safety, Proc. Inst. Mech. Eng. [H] 224 (2) (2010) 363–373, https://doi.org/10.1243/09544119JEIM613.
[30] A. Jerusalem, et al., Electrophysiological-mechanical coupling in the neuronal membrane and its role in ultrasound neuromodulation and general anaesthesia, Acta Biomater. 97 (Oct. 2019) 116–140, https://doi.org/10.1016/j.actbio.2019.07.041.
[31] B. Krasovitski, V. Frenkel, S. Shoham, E. Kimmel, Intramembrane cavitation as a unifying mechanism for ultrasound-induced bioeffects, Proc. Natl. Acad. Sci. USA 108 (8) (Feb. 2011) 3258–3263, https://doi.org/10.1073/pnas.1015771108.
[32] D. Dalecki, Mechanical bioeffects of ultrasound, Annu. Rev. Biomed. Eng. 6 (2004) 229–248, https://doi.org/10.1146/annurev.bioeng.6.040803.140126.
[33] G. Darmani, et al., Non-invasive transcranial ultrasound stimulation for neuromodulation, Clin. Neurophysiol. 135 (Mar. 2022) 51–73, https://doi.org/10.1016/j.clinph.2021.12.010.
[34] M.D. Menz, et al., Radiation force as a physical mechanism for ultrasonic neurostimulation of the ex vivo retina, J. Neurosci. Off. J. Soc. Neurosci. 39 (32) (Aug. 2019) 6251–6264, https://doi.org/10.1523/JNEUROSCI.2394-18.2019.
[35] A.G. Petrov, V.S. Sokolov, Curvature-electric effect in black lipid membranes, Eur. Biophys. J. 13 (3) (May 1986) 139–155, https://doi.org/10.1007/BF00542559.
[36] T.D. Nguyen, S. Mao, Y.-W. Yeh, P.K. Purohit, M.C. McAlpine, Nanoscale Flexoelectricity," Adv. Mater. 25 (7) (2013) 946–974, https://doi.org/10.1002/adma.201203852.
[37] S. Krichen, P. Sharma, Flexoelectricity: a perspective on an unusual electromechanical coupling, J. Appl. Mech. 83 (3) (Jan. 2016), https://doi.org/10.1115/1.4032378.
[38] A.G. Petrov, Flexoelectricity of model and living membranes, Biochim. Biophys. Acta BBA - Biomembr. 1561 (1) (Mar. 2002) 1–25, https://doi.org/10.1016/S0304-4157(01)00007-7.
[39] K. Yoon, et al., Effects of sonication parameters on transcranial focused ultrasound brain stimulation in an ovine model, PLoS One 14 (10) (2019), e0224311, https://doi.org/10.1371/journal.pone.0224311.
[40] J. Kubanek, P. Shukla, A. Das, S.A. Baccus, M.B. Goodman, Ultrasound elicits behavioral responses through mechanical effects on neurons and ion channels in a simple nervous system, J. Neurosci. Off. J. Soc. Neurosci. 38 (12) (Mar. 2018) 3081–3091, https://doi.org/10.1523/JNEUROSCI.1458-17.2018.
[41] P.N.T. Wells, Absorption and dispersion of ultrasound in biological tissue, Ultrasound Med. Biol. 1 (4) (Mar. 1975) 369–376, https://doi.org/10.1016/0301-5629(75)90124-6.
[42] M. Plaksin, S. Shoham, E. Kimmel, Intramembrane cavitation as a predictive bio-piezoelectric mechanism for ultrasonic brain stimulation, Phys. Rev. X 4 (1) (Jan. 2014), 011004, https://doi.org/10.1103/PhysRevX.4.011004.
[43] M. Plaksin, E. Kimmel, S. Shoham, Cell-type-selective effects of intramembrane cavitation as a unifying theoretical framework for ultrasonic neuromodulation, eNeuro 3 (3) (Jun. 2016), https://doi.org/10.1523/ENEURO.0136-15.2016. ENEURO.0136-15.2016.
[44] T. Lemaire, E. Neufeld, N. Kuster, S. Micera, Understanding ultrasound neuromodulation using a computationally efficient and interpretable model of intramembrane cavitation, J. Neural. Eng. 16 (4) (Aug. 2019), 046007, https://doi.org/10.1088/1741-2552/ab1685.
[45] T. Lemaire, E. Vicari, E. Neufeld, N. Kuster, S. Micera, MorphoSONIC: a morphologically structured intramembrane cavitation model reveals fiber-specific neuromodulation by ultrasound, iScience 24 (9) (Sep. 2021), 103085, https://doi.org/10.1016/j.isci.2021.103085.
[46] M.L. Prieto, K. Firouzi, B.T. Khuri-Yakub, M. Maduke, Activation of Piezo1 but not NaV1.2 channels by ultrasound at 43 MHz, Ultrasound Med. Biol. 44 (6) (Jun. 2018) 1217–1232, https://doi.org/10.1016/j.ultrasmedbio.2017.12.020.
[47] B. Sorum, R.A. Rietmeijer, K. Gopakumar, H. Adesnik, S.G. Brohawn, Ultrasound activates mechanosensitive TRAAK K+ channels through the lipid membrane, Proc. Natl. Acad. Sci. U.S.A. 118 (6) (Feb. 2021), e2006980118, https://doi.org/10.1073/pnas.2006980118.
[48] H. Chen, D. Garcia-Gonzalez, A. Jérusalem, Computational model of the mechanoelectrophysiological coupling in axons with application to neuromodulation, Phys. Rev. E 99 (3–1) (Mar. 2019), 032406, https://doi.org/10.1103/PhysRevE.99.032406.
[49] B.E. Treeby, B.T. Cox, k Wave, MATLAB toolbox for the simulation and reconstruction of photoacoustic wave fields, J. Biomed. Opt. 15 (2) (Apr. 2010), 021314, https://doi.org/10.1117/1.3360308.
[50] A.L. Hodgkin, A.F. Huxley, A quantitative description of membrane current and its application to conduction and excitation in nerve, J. Physiol. 117 (4) (Aug. 1952) 500–544.
[51] A.G. Petrov, Electricity and mechanics of biomembrane systems: flexoelectricity in living membranes, Anal. Chim. Acta 568 (1–2) (May 2006) 70–83, https://doi.org/10.1016/j.aca.2006.01.108.
[52] W.J. Tyler, The mechanobiology of brain function, Nat. Rev. Neurosci. 13 (12) (Dec. 2012) 867–878, https://doi.org/10.1038/nrn3383.
[53] A. Auerbach, The energy and work of a ligand-gated ion channel, J. Mol. Biol. 425 (9) (May 2013) 1461–1475, https://doi.org/10.1016/j.jmb.2013.01.027.
[54] J.K. Mueller, W.J. Tyler, A quantitative overview of biophysical forces impinging on neural function, Phys. Biol. 11 (5) (Aug. 2014), 051001, https://doi.org/10.1088/1478-3975/11/5/051001.

[55] Y. Meng, C.B. Pople, H. Lea-Banks, K. Hynynen, N. Lipsman, C. Hamani, Focused ultrasound neuromodulation, Int. Rev. Neurobiol. 159 (2021) 221–240, https://doi.org/10.1016/bs.irn.2021.06.004.
[56] M. Samandari, K. Abrinia, M. Mokhtari-Dizaji, A. Tamayol, Ultrasound induced strain cytoskeleton rearrangement: an experimental and simulation study, J. Biomech. 60 (Jul. 2017) 39–47, https://doi.org/10.1016/j.jbiomech.2017.06.003.
[57] J.B. Choi, S.H. Lim, K.W. Cho, D.H. Kim, D.P. Jang, I.Y. Kim, The effect of focused ultrasonic stimulation on the activity of hippocampal neurons in multi-channel electrode, in: 2013 6th International IEEE/EMBS Conference on Neural Engineering (NER), Nov. 2013, pp. 731–734, https://doi.org/10.1109/NER.2013.6696038.
[58] Z. Lin, et al., Ultrasound stimulation modulates voltage-gated potassium currents associated with action potential shape in hippocampal CA1 pyramidal neurons, Front. Pharmacol. 10 (2019) 544, https://doi.org/10.3389/fphar.2019.00544.
[59] M.L. Prieto, K. Firouzi, B.T. Khuri-Yakub, D.V. Madison, M. Maduke, Spike frequency-dependent inhibition and excitation of neural activity by high-frequency ultrasound, J. Gen. Physiol. 152 (11) (Nov. 2020), e202012672, https://doi.org/10.1085/jgp.202012672.
[60] Z. Cui, et al., Enhanced neuronal activity in mouse motor cortex with microbubbles' oscillations by transcranial focused ultrasound stimulation, Ultrason. Sonochem. 59 (Dec. 2019), 104745, https://doi.org/10.1016/j.ultsonch.2019.104745.
[61] J.A.N. Fisher, I. Gumenchuk, Low-intensity focused ultrasound alters the latency and spatial patterns of sensory-evoked cortical responses in vivo, J. Neural. Eng. 15 (3) (Mar. 2018), 035004, https://doi.org/10.1088/1741-2552/aaaee1.
[62] V. Colucci, G. Strichartz, F. Jolesz, N. Vykhodtseva, K. Hynynen, Focused ultrasound effects on nerve action potential in vitro, Ultrasound Med. Biol. 35 (10) (Oct. 2009) 1737–1747, https://doi.org/10.1016/j.ultrasmedbio.2009.05.002.
[63] E.J. Juan, R. González, G. Albors, M.P. Ward, P. Irazoqui, Vagus nerve modulation using focused pulsed ultrasound: potential applications and preliminary observations in a rat, Int. J. Imag. Syst. Technol. 24 (1) (Mar. 2014) 67–71, https://doi.org/10.1002/ima.22080.
[64] B. F, M. B, S. R, G. H, Transcranial focused ultrasound modulates electrical behavior of the neurons: design and implementation of a model, J. Biomed. Phys. Eng. 10 (1) (Feb. 2020) 65–74, https://doi.org/10.31661/jbpe.v0i0.1052.
[65] H. Guo, et al., Ultrasound does not activate but can inhibit in vivo mammalian nerves across a wide range of parameters, Sci. Rep. 12 (1) (Feb. 2022), https://doi.org/10.1038/s41598-022-05226-7. Art. no. 1.
[66] B. Howell, L.E. Medina, W.M. Grill, Effects of frequency-dependent membrane capacitance on neural excitability, J. Neural. Eng. 12 (5) (Oct. 2015), https://doi.org/10.1088/1741-2560/12/5/056015, 056015–056015.
[67] P.N.T. Wells, H.-D. Liang, Medical ultrasound: imaging of soft tissue strain and elasticity, J. R. Soc. Interface 8 (64) (Nov. 2011) 1521–1549, https://doi.org/10.1098/rsif.2011.0054.
[68] R.M. Almasri, W. AlChamaa, A.R. Tehrani-Bagha, M.L. Khraiche, Highly flexible single-unit resolution all printed neural interface on a bioresorbable backbone, ACS Appl. Bio Mater. 3 (10) (Oct. 2020) 7040–7051, https://doi.org/10.1021/acsabm.0c00895.
[69] S. Ha, M.L. Khraiche, G.A. Silva, G. Cauwenberghs, Direct inductive stimulation for energy-efficient wireless neural interfaces, in: Proceedings of the Annual International Conference of the IEEE Engineering in Medicine and Biology Society, EMBS, 2012, https://doi.org/10.1109/EMBC.2012.6346073.